A Simulation of the Separate Climate Effects of Middle-Atmospheric and Tropospheric CO_2 Doubling

M. SIGMOND

Department of Applied Physics, Eindhoven University of Technology (TUE), Eindhoven, and Royal Netherlands Meteorological Institute (KNMI), De Bilt, Netherlands

P. C. SIEGMUND

Royal Netherlands Meteorological Institute (KNMI), De Bilt, Netherlands

E. MANZINI

Istituto Nazionale di Geofisica e Vulcanologia, Bologna, Italy

H. KELDER

Department of Applied Physics, Eindhoven University of Technology (TUE), Eindhoven, and Royal Netherlands Meteorological Institute (KNMI), De Bilt, Netherlands

(Manuscript received 14 July 2003, in final form 27 November 2003)

ABSTRACT

The separate climate effects of middle-atmospheric and tropospheric CO_2 doubling have been simulated and analyzed with the ECHAM middle-atmosphere climate model. To this end, the CO_2 concentration has been separately doubled in the middle-atmosphere, the troposphere, and the entire atmosphere, and the results have been compared to a control run. During NH winter, the simulated uniformly doubled CO_2 climate shows an increase of the stratospheric residual circulation, a small warming in the Arctic lower stratosphere, a weakening of the zonal winds in the Arctic middle-atmosphere, an increase of the NH midlatitude tropospheric westerlies, and a poleward shift of the SH tropospheric westerlies. The uniformly doubled CO_2 response in most regions is approximately equal to the sum of the separate responses to tropospheric and middle-atmospheric CO_2 doubling. The increase of the stratospheric residual circulation can be attributed for about two-thirds to the tropospheric CO_2 doubling and one-third to the middle-atmospheric CO_2 doubling. This increase contributes to the Arctic lower-stratospheric warming and, through the thermal wind relationship, to the weakening of the Arctic middle-atmospheric zonal wind. The increase of the tropospheric NH midlatitude westerlies can be attributed mainly to the middle-atmospheric CO_2 doubling, indicating the crucial importance of the middle-atmospheric CO_2 doubling for the tropospheric climate change. Results from an additional experiment show that the CO_2 doubling above 10 hPa, which is above the top of many current GCMs, also causes significant changes in the tropospheric climate.

1. Introduction

The notion that the stratosphere influences the troposphere has been supported by many recent studies. Low-frequency zonal wind variations propagate downward from the upper stratosphere to the lower troposphere (e.g., Kodera et al. 1990). Anomalies in the leading mode of variability of the Northern Hemispheric (NH) circulation [known as either the Arctic Oscillation (AO) or the Northern Hemisphere annular mode (NAM): Thompson and Wallace 1998] generally first appear in the stratosphere and propagate to the surface within several weeks (Baldwin and Dunkerton 1999). Several dynamical mechanisms for this downward propagation have been proposed: potential vorticity induction (Hartley et al. 1998), wave–mean flow interactions (e.g., Shindell et al. 2001) and meridional mass redistribution (Sigmond et al. 2003). During the last 30 years, the index corresponding to this leading mode of variability (the AO index) has undergone a positive trend, which can explain about 50% of the observed surface temperature increase over the Eurasian continent (Thompson et al. 2000). Since the AO is related to the midlatitude stratospheric zonal wind (e.g., Thompson et al. 2000), the observed warming may be partially due to changes in the stratospheric circulation. Several GCM studies predict an in-

Corresponding author address: Dr. M. Sigmond, KNMI, P.O. Box 201, 3730 AE, De Bilt, Netherlands.
E-mail: sigmond@knmi.nl

creased westerly circulation in the (lower) tropospheric NH midlatitudes (associated with a further increase of the AO index) in response to increasing CO_2 concentrations (Shindell et al. 1999; Fyfe et al. 1999; Paeth et al. 1999; Gillett et al. 2002). The increase of greenhouse gases is believed to cool the polar stratosphere, to warm the tropical upper troposphere and, consequently, to increase the meridional temperature gradient in the tropopause region. Shindell et al. (2001) argue that this causes stratospheric zonal wind changes that in turn cause the increased westerly circulation in the tropospheric NH midlatitudes through wave–mean flow interactions. Several other GCM studies also indicate this downward influence (Boville 1984; Rind et al. 2002).

Other recent studies have addressed the question of how well the stratosphere has to be represented in GCMs to capture this downward influence adequately. Shindell et al. (1999) show that their model only captures the observed AO index increase if it includes the region between 10 and 0.01 hPa. However, Fyfe et al. (1999) and Gillett et al. (2002) found an AO index increase in response to increasing CO_2 concentrations in models with an upper boundary at, respectively, 12 and 5 hPa. The latter result did not notably change when the upper boundary was raised to 0.01 hPa.

Greenhouse-gas-induced changes in the troposphere are expected to change the stratospheric circulation. Tropospheric waves propagate upward into the stratosphere, where they are dissipated and drive a meridional overturning circulation, known as the residual or Brewer–Dobson circulation (e.g., Holton et al. 1995). Tropospheric greenhouse gas increases can alter the sources and propagation patterns of the atmospheric waves that drive the stratospheric residual circulation. In a GCM experiment with increasing CO_2, Butchart and Scaife (2001) found an increase of the strength of this circulation. They argued that such an increase would accelerate the removal of chlorofluorocarbons (CFCs) from the stratosphere and, consequently, accelerate the recovery of the ozone layer.

Rind et al. (1990) investigated the causes of the middle-atmospheric response to a uniform doubling of CO_2, by performing experiments of one to three years timescale in which the CO_2 was doubled in either the middle-atmosphere or the troposphere. They suggested that the residual stratospheric circulation increase is due to both the ''in situ'' (middle-atmospheric) and the ''remote'' (tropospheric) CO_2 doubling. The tropospheric response to CO_2 doubling in either the troposphere or middle-atmosphere was not considered in this study.

In the present study, the separate climate effects of middle-atmospheric and tropospheric CO_2 increase are investigated with the middle-atmosphere version of the ECHAM global climate model. The control and uniformly doubled CO_2 climate have been simulated. In addition, experiments have been performed in which the CO_2 has been doubled in either the troposphere or the middle-atmosphere. These idealized experiments have been performed to study the mechanisms leading to the changes in the simulated uniformly doubled CO_2 climate. Changes found in the uniformly doubled CO_2 climate will be attributed to either middle-atmospheric or tropospheric CO_2 doubling. We will investigate whether this separation is allowed, which requires that the response to a uniform CO_2 doubling is approximately equal to the sum of the separate responses to tropospheric and middle-atmospheric CO_2 doubling. We have performed 30-yr equilibrium experiments to obtain statistically significant results. Since the stratosphere–troposphere coupling is strongest in NH winter, we will focus on this season.

This paper is organized as follows. In section 2 the model and the setup of the experiments are described. In section 3 the control climate and the response to a uniform CO_2 doubling is described. The climate responses to nonuniform (i.e., only tropospheric or middle-atmospheric) CO_2 doubling are described in section 4. It is investigated to what extent the response to a uniform CO_2 doubling can indeed be regarded as the sum of the responses to tropospheric and middle-atmospheric CO_2 doubling. The downward influence of middle-atmospheric CO_2 doubling on the troposphere is investigated in more detail in section 5. Finally, the results are summarized and discussed in section 6.

2. Model and setup of the experiments

a. The general circulation model

The GCM used in this study is MA-ECHAM4 (Manzini et al. 1997), which is the middle-atmosphere version of the ECHAM4 model (Roeckner et al. 1996). The MA-ECHAM4 model has 39 levels from the surface up to 0.01 hPa (about 80 km). Gravity wave drag is parameterized for both orographic gravity waves (McFarlane 1987) and a spectrum of nonstationary gravity waves (Hines 1997a,b). Sensitivities to the specification of the gravity wave parameterizations are discussed by Manzini and McFarlane (1998). The simulations in this study are performed at T42 horizontal resolution (about $2.8° \times 2.8°$) and the integration time step is set to 10 minutes. The ozone distribution (Brühl 1993) and the sea surface temperatures (SSTs) are prescribed.

b. Experiments

Six 30-yr simulations have been performed, whose configurations are summarized in Table 1. The atmospheric CO_2 content has been doubled in the entire atmosphere from 353 ppmv in the control run (C run) to 706 ppmv in the uniformly doubled CO_2 run (A run). Two additional runs have been performed in which the CO_2 is separately doubled in the middle-atmosphere (M run) and the troposphere (T run). A monthly mean, longitude- and latitude-dependent tropopause field was used to select the regions where CO_2 should be doubled

TABLE 1. Summary of the configurations of the experiments, see section 2b.

	C-run	A-run	M-run	T-run	MC-run	H-run
Middle Atmosphere	1X CO_2	2x CO_2	2x CO_2	1X CO_2	2x CO_2	2x CO_2 (only above 10 hPa)
Troposphere	1X CO_2	2x CO_2	1X CO_2	2x CO_2	1X CO_2	1X CO_2
SST	Control	2x CO_2	RF-calculation	RF-Calculation	Control	Control

in the M and T runs. This climatology was calculated with the WMO tropopause definition and was taken from a control run of MA-ECHAM4.

The atmospheric GCM is not interactively coupled to an ocean model. Instead, monthly climatological SSTs are prescribed. In the C and A runs these SSTs are taken from a control and a doubled CO_2 run of ECHAM4 coupled to a slab layer ocean. The appropriate SSTs in the M and T runs were calculated from these climatologies and calculated radiative forcings. The radiative forcing (RF) is the net radiative flux change at the tropopause caused by a radiative perturbation (e.g., Houghton et al. 2001), and is generally considered as a useful measure for the surface temperature change. It is assumed that

$$\mathrm{RF_A} = \mathrm{RF_M} + \mathrm{RF_T}, \tag{1a}$$

where $\mathrm{RF_X}$ is the radiative forcing due to the CO_2 doubling in region X (M for middle-atmosphere, T for troposphere, and A for the entire atmosphere) and that the climate sensitivity parameter λ ($=\mathrm{RF}/\Delta T_{\mathrm{surf}}$) is the same for each $\mathrm{RF_X}$. Under these conditions, it can be derived that

$$\Delta\mathrm{SST_T} = \Delta\mathrm{SST_A} \times \mathrm{frac}, \tag{1b}$$

$$\Delta\mathrm{SST_M} = \Delta\mathrm{SST_A} \times (1 - \mathrm{frac}), \tag{1c}$$

where

$$\mathrm{frac} = \frac{\mathrm{RF_T}}{\mathrm{RF_T} + \mathrm{RF_M}}. \tag{1d}$$

The $\Delta\mathrm{SST_X}$ is the change of SST compared to the control run due to the CO_2 doubling in region X. To compute $\mathrm{RF_X}$, we have performed three additional integrations with the configurations of the M, T, and A runs, except that the control SSTs are prescribed. Here $\mathrm{RF_X}$ is approximated by the global-mean net radiative flux change at the tropopause compared to the control run after one time step. From the results ($\mathrm{RF_M} = 0.64$ W m^{-2}, $\mathrm{RF_T} = 3.26$ W m^{-2}) a value of 0.84 for frac is obtained. Since $\mathrm{RF_A} = 3.89$ W m^{-2}, Eq. (1a) appears to be valid almost exactly. Since frac is close to unity, the sea ice distribution in the M run is prescribed to be equal to that in the C run whereas the sea ice distribution in the T run is equal to that in the A run. The approach that we use is relatively simple because the possible dependency of λ on the vertical location of the CO_2 forcing is not considered and we calculated frac from instantaneous radiative forcings, whereas it would have been more appropriate to calculate it from the adjusted radiative forcings.

To investigate to what extent the imposed SST changes in the M run influence the results, an additional run (denoted as the MC run) has been performed, which is similar to the M run except that the control SSTs are prescribed.

To investigate the influence of the CO_2 doubling in the higher stratosphere and mesosphere on the tropospheric climate, a run has been performed in which the CO_2 is doubled only above 10 hPa (H run). The radiative forcing due to the CO_2 doubling above 10 hPa is calculated in the same way as for the other runs and was found to be very small (0.02 W m^{-2}). Therefore, control SSTs could be imposed in the H run.

3. The climate response to a uniform CO_2 doubling

a. The control climate

Figures 1a and 1b show, respectively, the zonally averaged temperature and zonal wind in the control climate in NH winter. The temperature distribution, the strength of the NH stratospheric polar vortex, the subtropical jet streams, and the SH middle-atmospheric easterlies compare reasonably well with reference climatologies (Manzini and McFarlane 1998) except that the position of the polar vortex wind maximum (60°N) is a bit too far poleward. The residual mean streamfunction [computed following the transformed Eulerian mean formulation (Andrews et al. 1987)] depicted in Fig. 1c shows the stratospheric residual circulation. This circulation is driven by the wave drag from planetary and gravity waves. The planetary waves are resolved by the model

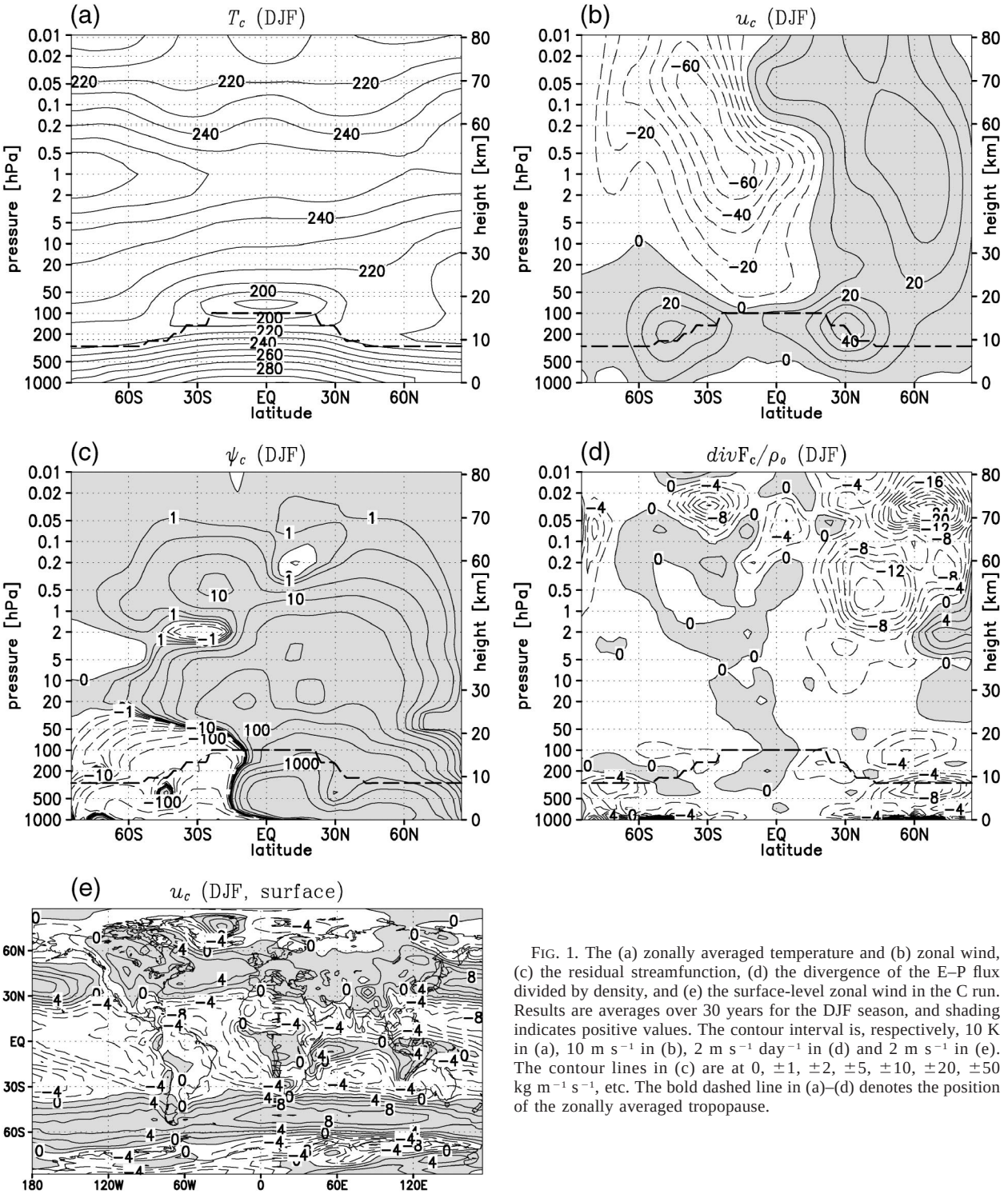

FIG. 1. The (a) zonally averaged temperature and (b) zonal wind, (c) the residual streamfunction, (d) the divergence of the E–P flux divided by density, and (e) the surface-level zonal wind in the C run. Results are averages over 30 years for the DJF season, and shading indicates positive values. The contour interval is, respectively, 10 K in (a), 10 m s^{-1} in (b), 2 m s^{-1} day^{-1} in (d) and 2 m s^{-1} in (e). The contour lines in (c) are at 0, ±1, ±2, ±5, ±10, ±20, ±50 kg m^{-1} s^{-1}, etc. The bold dashed line in (a)–(d) denotes the position of the zonally averaged tropopause.

and their effect on the mean flow is quantified by div$\mathbf{F}/\rho_0$ [where div$\mathbf{F}$ is the divergence of the Eliassen–Palm (E–P) flux and ρ_0 is the density], which is shown in Fig. 1d. In regions where div$\mathbf{F}/\rho_0$ is negative, the waves decelerate the zonal wind, thus causing an imbalance between the Coriolis force on the zonal-mean zonal wind and the meridional pressure gradient force, driving a poleward flow. The surface zonal wind (Fig. 1e) is largest in the northern Atlantic and Pacific storm track regions and in the SH midlatitudes.

In this paper, we will focus on the December–February (DJF) season, that is, NH winter and SH summer. In this season the zonal wind in the SH middle-atmosphere is easterly (Fig. 1a), constituting a barrier for the transport of tropospheric wave activity into the middle-atmosphere (Charney and Drazin 1961). Consequently, in this season no strong stratosphere–troposphere interactions are expected in the Southern Hemisphere, in contrast to in the Northern Hemisphere. Therefore, the differences between the Northern and the Southern Hemisphere discussed in this paper are not caused by hemispheric differences, but by seasonal differences.

b. The middle-atmospheric response to uniform CO_2 doubling

Figure 2a shows the zonally averaged temperature difference between the A run and the C run in NH winter (denoted as ΔT_A). As expected, the middle-atmosphere generally cools in response to the uniform CO_2 doubling, which can be explained by radiative arguments (e.g., Fels et al. 1980; Shindell et al. 2001). The changes are statistically significant, except in some regions where the changes are small. The main exception to the middle-atmospheric cooling is the Arctic lower stratosphere, which slightly warms. Figure 2b shows the zonally averaged zonal wind difference between the A and the C run in NH winter (Δu_A), which is physically consistent with Fig. 2a according to the thermal wind relationship. The warming of the Arctic lower stratosphere and the reduced cooling directly above this layer lead to a decrease of the meridional temperature gradient in the polar stratosphere, consistent with the weakening of the Arctic middle-atmospheric zonal winds. The zonal wind in the NH subtropical middle-atmosphere strengthens, with up to 9 m s^{-1} near the stratopause and just above the NH subtropical jet stream. The position of the maximum wind speed in the polar vortex has shifted equatorward from 60°N in the C run to 40°N in the A run, and its value has decreased from 38 m s^{-1} in the C run to 34 m s^{-1} in the A run (not shown). In the Southern Hemisphere, the middle-atmospheric extratropical easterlies significantly decrease in magnitude.

Figure 2c shows the change of the residual streamfunction in the A run compared to the C run ($\Delta\psi_A$). The strength of the stratospheric residual circulation generally increases except in the tropical middle stratosphere. The maximum of the NH residual streamfunction, which is located between 15° and 18°N and is a measure for the NH extratropical mass flux from the stratosphere to the troposphere (e.g., Rosenlof and Holton 1993), significantly increases 33% at 50 hPa and 39% at 100 hPa. Associated with this increase, the descending motions near the North Pole increase. While adiabatically heating the air, they contribute to the temperature increase shown in Fig. 2a.

To get an idea of the causes of the increased NH extratropical residual circulation, the change of the residual meridional wind is investigated. Figure 3a shows for the A run in the NH extratropics the change of the residual meridional wind, from which the streamfunction change depicted in Fig. 2c has been computed. This residual meridional wind is defined as [Andrews et al. 1987, Eq. (3.5.1a)]

$$v^* \equiv \overline{v} - \rho_0^{-1}\frac{\partial[\rho_0\overline{v'\theta'}(\partial\overline{\theta}/\partial z)^{-1}]}{\partial z}, \tag{2}$$

where ρ_0 is the density, v is meridional wind, and θ is the potential temperature. The overbar denotes the zonal-mean value; the prime denotes the deviation from that value. Figure 3a shows that in most of the NH extratropical stratosphere v^* increases in the doubled CO_2 climate, which corresponds to the increased residual circulation. Figure 3b shows the part of Δv_A^* that is due to resolved waves (denoted as $\Delta v_A^{*,\text{resolved}}$). The $v^{*,\text{resolved}}$ has been computed by applying the continuity equation to the vertical velocity due to planetary wave driving, assuming ''downward control'' (Haynes et al. 1991). Since the analysis is focused on the extratropics, the quasigeostrophic approximation can be applied. Assuming quasigeostrophy and stationarity, this vertical velocity can be written as

$$w^{*,\text{resolved}} = \frac{1}{a\rho_0\cos\phi}\frac{\partial}{\partial\phi}\left[\int_z^\infty \left(\frac{\cos\phi\ \text{div}\mathbf{F}}{f}\right)_{\phi=\text{const.}} dz'\right], \tag{3}$$

where a is the radius of the earth, ϕ is latitude, and f is the Coriolis parameter. Comparison of Figs. 3b and 4a for the resolved waves shows that the structure of $\Delta v_A^{*,\text{resolved}}$ is opposite to that of $\Delta\text{div}\mathbf{F}_A/\rho_0$. The decreased (i.e., more negative) $\text{div}\mathbf{F}_A/\rho_0$ in the large part of the NH stratosphere implies that the wave drag due to the resolved waves on the zonally averaged zonal flow increases, and that the resolved waves strengthen the poleward flow (i.e., $v^{*,\text{resolved}}$ increases).

In the extratropical stratosphere and mesosphere, changes in the direct thermally forced component of v^* are expected to be small. Therefore, the part of the change in v^* that is not due to resolved waves (denoted as $\Delta v_A^{*,\text{residual}}$) in these regions is expected to be mainly due to unresolved gravity waves. In the NH midlatitude stratosphere $\Delta v_A^{*,\text{residual}}$ is comparable to $\Delta v_A^{*,\text{resolved}}$. In some stratospheric regions (e.g., region 1) Δv_A^* is even mainly due to $\Delta v_A^{*,\text{residual}}$. Therefore, it is concluded that changes in both the resolved waves and other processes (of which gravity waves are expected to be the most important) drive the increased stratospheric NH extratropical residual circulation in the doubled CO_2 climate. In the mesosphere, planetary wave activity is very small due to absorption of these waves at lower levels, which

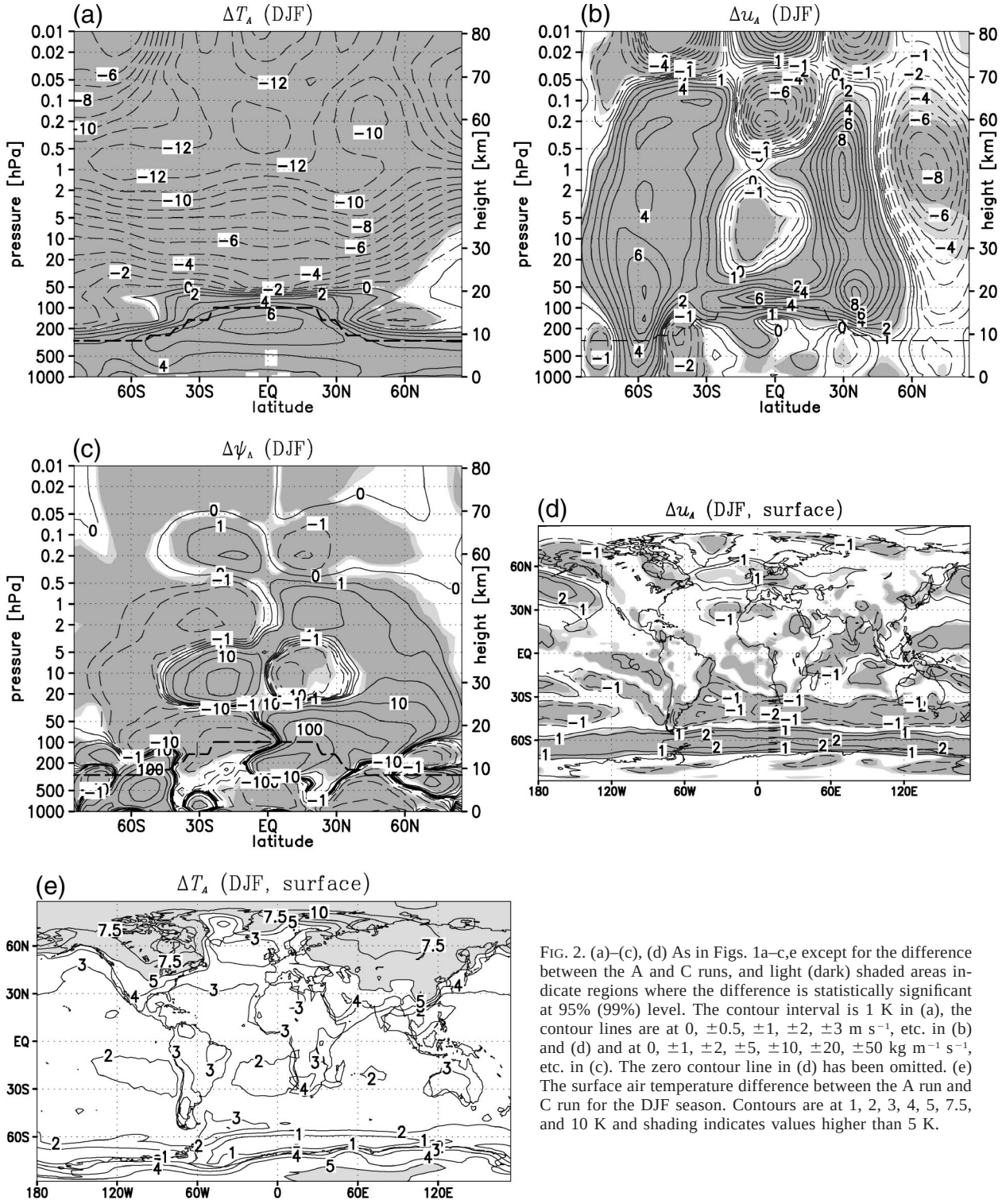

FIG. 2. (a)–(c), (d) As in Figs. 1a–c,e except for the difference between the A and C runs, and light (dark) shaded areas indicate regions where the difference is statistically significant at 95% (99%) level. The contour interval is 1 K in (a), the contour lines are at 0, ±0.5, ±1, ±2, ±3 m s^{-1}, etc. in (b) and (d) and at 0, ±1, ±2, ±5, ±10, ±20, ±50 kg m^{-1} s^{-1}, etc. in (c). The zero contour line in (d) has been omitted. (e) The surface air temperature difference between the A run and C run for the DJF season. Contours are at 1, 2, 3, 4, 5, 7.5, and 10 K and shading indicates values higher than 5 K.

can explain why in this region $\Delta v_A^{*,\text{resolved}}$ is generally smaller than $\Delta v_A^{*,\text{residual}}$. Thus, the mesospheric Δv_A^* is mainly determined by gravity waves drag changes.

Figure 4a shows that in the NH stratosphere the pattern of the $\Delta \text{div}\mathbf{F}_A/\rho_0$ is similar to that of Δu_A (Fig. 2b): they both decrease in the polar region and increase around 40°N. This finding is consistent with the fact that $\text{div}\mathbf{F}/\rho_0$ is a force on the zonal-mean zonal wind.

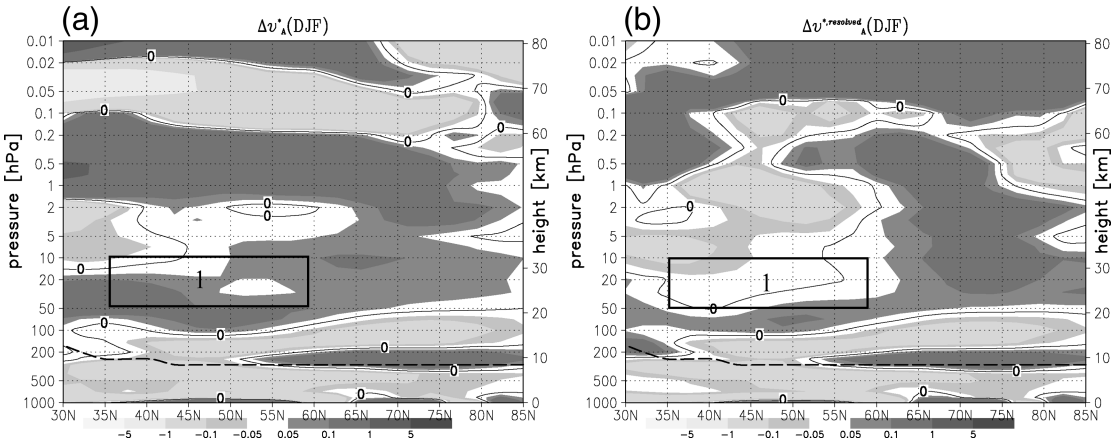

FIG. 3. The difference between the A and C runs of (a) v^* and (b) $v^{*,\text{resolved}}$, for NH winter. The zero contour line is plotted. See section 3b for the meaning of the symbols. Only the NH extratropics are plotted.

The changes in the resolved waves are investigated in more detail by decomposing $\text{div}\mathbf{F}/\rho_0$ in its horizontal and vertical components $\text{div}\mathbf{F}^y/\rho_0$ and $\text{div}\mathbf{F}^z/\rho_0$, which in the quasigeostrophic approximation are given by

$$\text{div}\mathbf{F}^y = \frac{\partial}{\partial y}F^y, \tag{4a}$$

$$\text{div}\mathbf{F}^z = \frac{\partial}{\partial z}F^z, \tag{4b}$$

$$F^y = -\rho_0\overline{u'v'}, \tag{4c}$$

$$F^z = \rho_0 fa\cos\phi\overline{v'\theta'}(\partial\overline{\theta}/\partial z)^{-1}. \tag{4d}$$

Here F^y and F^z are, respectively, the horizontal and vertical component of the Eliassen–Palm flux vector, which is in the direction of the wave activity: F^z is generally positive, corresponding to an upward propagation of the wave activity, and a positive F^y corresponds to a poleward propagation of wave activity. Figure 4 shows that in the NH upper stratosphere (region I) and in the NH subtropical lower stratosphere (region II) the structure of $\Delta\text{div}\mathbf{F}_A/\rho_0$ (Fig. 4a, shaded) is mainly determined by $\Delta\text{div}\mathbf{F}^y_A/\rho_0$ (Fig. 4b, shaded), whereas in the NH midlatitude middle stratosphere (region III) it is mainly determined by $\text{div}\mathbf{F}^z/\rho_0$ (Fig. 4c, shaded). Changes in $\text{div}\mathbf{F}^y/\rho_0$ are related to changes in F^y and, consequently, to changes in the meridional refraction of wave activity. For example, in the middle of region II F^y (Fig. 4b, contours) decreases, implying that waves are refracted more to the equator (see arrow), leading to decreases of $\text{div}\mathbf{F}^y/\rho_0$ at the equatorward side of region II and increases of $\text{div}\mathbf{F}^y/\rho_0$ at the poleward side of region II. Changes in $\text{div}\mathbf{F}^z/\rho_0$ are related to changes in F^z and, consequently, to changes in the vertical prop-

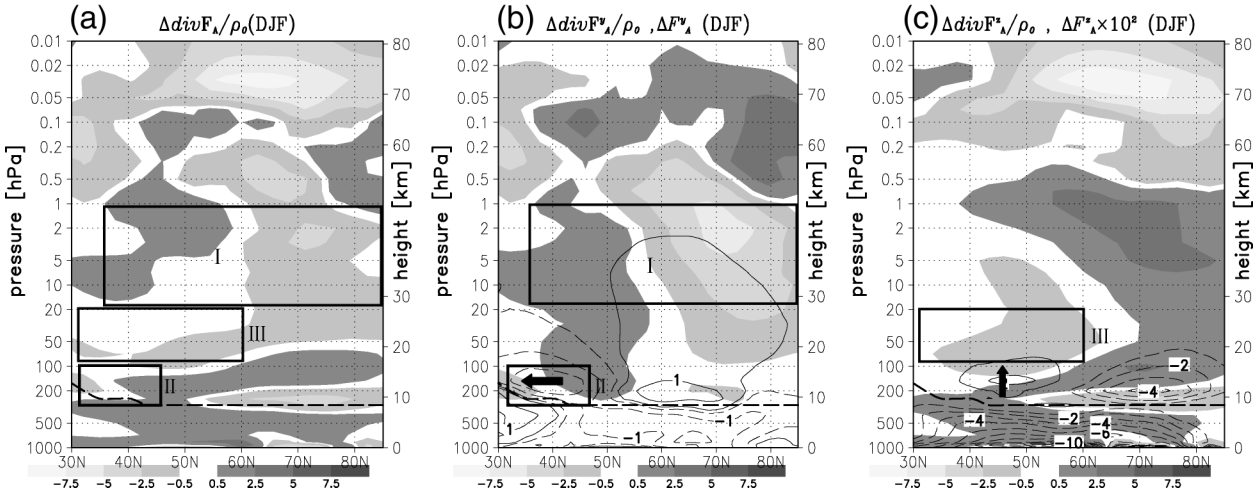

FIG. 4. The difference between the A and C runs in NH winter of (a) $\text{div}\mathbf{F}/\rho_0$, (b) $\text{div}\mathbf{F}^y/\rho_0$ (shaded) and F^y (contours), (c) $\text{div}\mathbf{F}^z/\rho_0$ (shaded) and $F^z \times 10^2$ (contours). See text for the meaning of the symbols. Here, $\text{div}\mathbf{F}/\rho_0$ is in m s^{-1} day^{-1}. The contour lines of F^y are at ± 0.2, ± 1, ± 2, ± 3 Pa, etc. and the contour interval of F^z is 0.01 Pa. The zero contour lines for both F^y and F^z are omitted. The arrows indicate the directions of the changes of the wave propagation discussed in the text. Only the NH extratropics are plotted.

agation of the wave activity. Just below region III F^z (Fig. 4c, contours) increases, which corresponds to more upward propagating wave activity (see upward arrow). This increased wave activity is dissipated in region III, causing a decrease of $\text{div}\mathbf{F}^z/\rho_0$. In summary, the structure of $\Delta\text{div}\mathbf{F}_A/\rho_0$ is mainly determined by changes in the meridional refraction of the wave activity in the NH upper stratosphere (region I) and in the NH subtropical lower stratosphere (region II), and by the increase of vertical wave activity in the NH midlatitude lower stratosphere (just below region III). Considering that the tropospheric vertical wave activity is decreased (see Fig. 4c), the lower-stratospheric increase can have two causes: 1) the NH midlatitude tropopause is more ''transparent'' for tropospheric wave activity or 2) more wave activity is produced near the NH midlatitude tropopause.

The Arctic lower-stratospheric warming in response to CO_2 increase (Fig. 2a) has been reported in several GCM studies (e.g., Rind et al. 1990, 1998, 2002; Mahfouf et al. 1994; Gillett et al. 2003). An exception is the study of Shindell et al. (1998) who report a cooling of the polar vortex [see Gillett et al. (2003) for a discussion]. Gillet et al. also found a weakening of the polar vortex whereas other studies (e.g., Rind et al. 1998; Shindell et al. 1998) found indications for a strengthening of the vortex. In the present study the Arctic lower-stratospheric warming is attributed to an increased residual circulation due to increased planetary and gravity wave driving. It should be noted that the change in the upward propagation of vertical wave energy quantified by ΔF^z_A at 100 hPa was found to be largest in November, causing a huge deceleration of the polar vortex compared to the control run, and influencing the strength of the polar vortex in the succeeding winter. Thus, the strength of the DJF polar vortex is not only influenced by the DJF wave activity, but also by that in November. The increase of the NH midlatitude lower-stratospheric wave driving in NH winter is consistent to what has been found by, for example, Butchart and Scaife (2001) and Gillett et al. (2003). In the NH subtropical lower stratosphere, the increased wave driving is due to the equatorward refraction of wave activity, which is consistent with the results of, for example, Rind et al. (2002).

c. The tropospheric response to uniform CO_2 doubling

Figure 2a shows that the troposphere generally warms in response to a uniform CO_2 doubling, with a maximum warming of more than 6 K in the tropical upper troposphere. Figure 2b shows that the zonally averaged zonal wind in the tropospheric NH midlatitudes increases 0.5 to 1 m s^{-1}. At the surface (Fig. 2d), these significant zonal wind increases are found in the storm track regions above the oceans. Above the northern Atlantic, the zonal wind increases more than 1.5 m s^{-1}, which is about 20% of the zonal wind in the C run. The increase of the tropospheric NH midlatitude westerlies has been reported in several previous GCM studies (see section 1). The decrease of the zonal wind around 40°S and the increase around 60°S throughout the troposphere imply that the SH summer westerlies are shifted poleward. Figure 2e shows the surface air temperature change in response to a uniform CO_2 doubling. It shows that the surface air temperature generally increases 2–3 K, except at high latitudes, where the temperature increases up to 12 K due to the high-latitude warming amplification.

To summarize, the simulated uniformly doubled CO_2 climate is characterized by a generally cooler middle-atmosphere, an increased stratospheric residual circulation (caused by increased planetary and gravity wave driving) that is consistent with warmer temperatures in the Arctic lower stratosphere and a weakening of the zonal winds in the Arctic middle-atmosphere. Furthermore, the troposphere warms and the tropospheric NH midlatitude westerlies increase.

4. The climate response to nonuniform CO_2 doubling

Experiments in which the CO_2 is doubled nonuniformly (i.e., only in the troposphere or in the middle-atmosphere) have been performed to study the mechanisms leading to the changes in the simulated uniformly doubled CO_2 climate. Changes found in the uniformly doubled CO_2 climate are attributed to either middle-atmospheric or tropospheric CO_2 doubling. This separation is only allowed when the responses are additive, that is, when the response to a uniform CO_2 doubling can be regarded as the sum of the responses to CO_2 doubling in the middle-atmosphere and in the troposphere. In other words, the following relationship should apply:

$$\Delta Q_A = \Delta Q_M + \Delta Q_T, \tag{5}$$

where ΔQ_X is the response to CO_2 doubling in region X (i.e., the difference between the X run and the C run) of the quantity Q. Relationship (5) will generally not be satisfied exactly due to nonlinear middle-atmosphere–troposphere interactions. It will be assumed that the responses are additive if relationship (5) applies at a more than 95% confidence level. A Student's t test is applied to $(\Delta Q_M + \Delta Q_T - \Delta Q_A)$ to test whether this quantity significantly differs from zero. Significant nonadditives arise in regions where the value of $(\Delta Q_M + \Delta Q_T - \Delta Q_A)$ is large or where its interannual variability is small.

a. The middle-atmospheric response

Figure 5 shows for NH winter the zonally averaged temperature response to middle-atmospheric CO_2 doubling (ΔT_M, Fig. 5a) and to tropospheric CO_2 doubling (ΔT_T, Fig. 5b). Figure 5c shows that the temperature

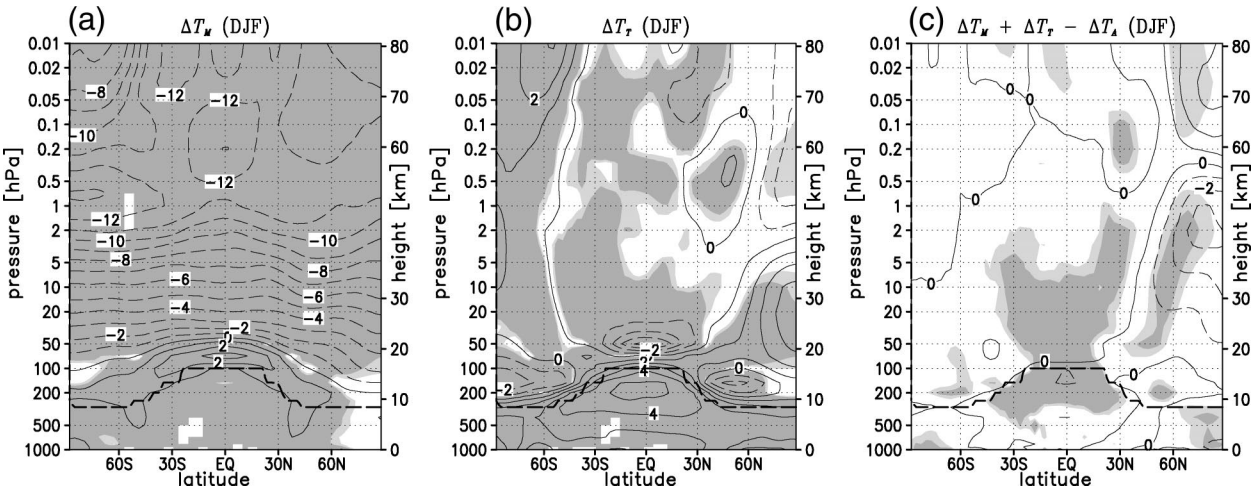

FIG. 5. The difference of the zonally averaged temperature between (a) the M and C runs and (b) the T and C runs for the DJF season. (c) The degree of nonadditivity of the temperature (i.e., $\Delta T_M + \Delta T_T - \Delta T_A$, see text). Light (dark) shading denotes significance at 95% (99%) level of the changes in (a) and (b) and of the nonadditivity in (c). The contour interval is 1 K. The bold dashed line denotes the position of the tropopause.

changes satisfy additiveness (i.e., $\Delta T_M + \Delta T_T - \Delta T_A \approx 0$) in the largest part of the middle-atmosphere, except in some regions (shaded when not additive), which includes the tropical and part of the NH extratropical stratosphere. Note that the temperature responses are additive in the Arctic lower and middle stratosphere. Figure 6 shows the zonally averaged zonal wind response to middle-atmospheric CO_2 doubling (Δu_M, Fig. 6a) and to tropospheric CO_2 doubling (Δu_T, Fig. 6b) in NH winter. The shaded regions in Fig. 6c indicate regions where the zonal wind responses are not additive.

Figure 5b shows that in the largest part of the middle-atmosphere the temperature response to tropospheric CO_2 doubling (ΔT_T) is small. This is not surprising considering that the CO_2 concentration in the T run is not doubled in the middle-atmosphere so that direct radiative effects are absent. However, a statistically significant warming of more than 3 K in the Arctic lower stratosphere (maximum at 20 hPa) and a statistically significant cooling of more than 2 K in the tropical lower stratosphere (maximum at 50 hPa) is found. In the middle-atmosphere, Δu_T is similar to Δu_A (Fig. 2b): they both are positive in the Arctic and negative in the subtropics. Figure 7b shows the change in the residual streamfunction in the T run. Similar to what was found in the A run, the residual circulation in the T run strengthens in most of the NH lower and middle stratosphere. However, different from what was found in the A run, the residual streamfunction does not increase in the NH upper stratosphere and mesosphere. The maximum of the NH residual streamfunction increases 18% at 50 hPa and 26% at 100 hPa. These changes are ap-

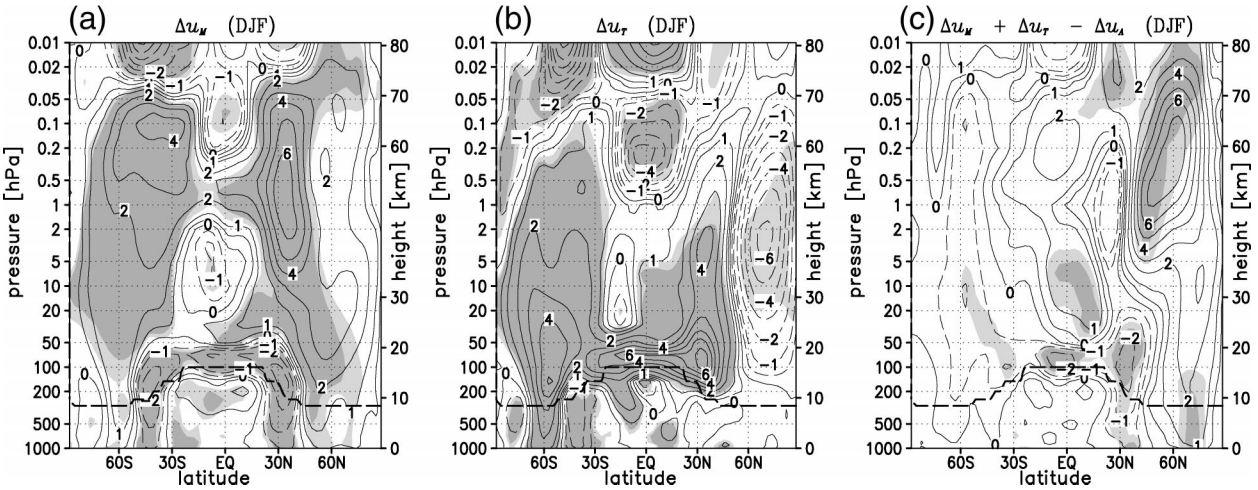

FIG. 6. As in Figs. 5a–c except for the zonally averaged zonal wind. The contour lines are at 0, ±0.5, ±1, ±2, ±3 m s^{-1}, etc. Light (dark) shading denotes significance at 95% (99%) level of the changes in (a) and (b) and of the nonadditivity in (c).

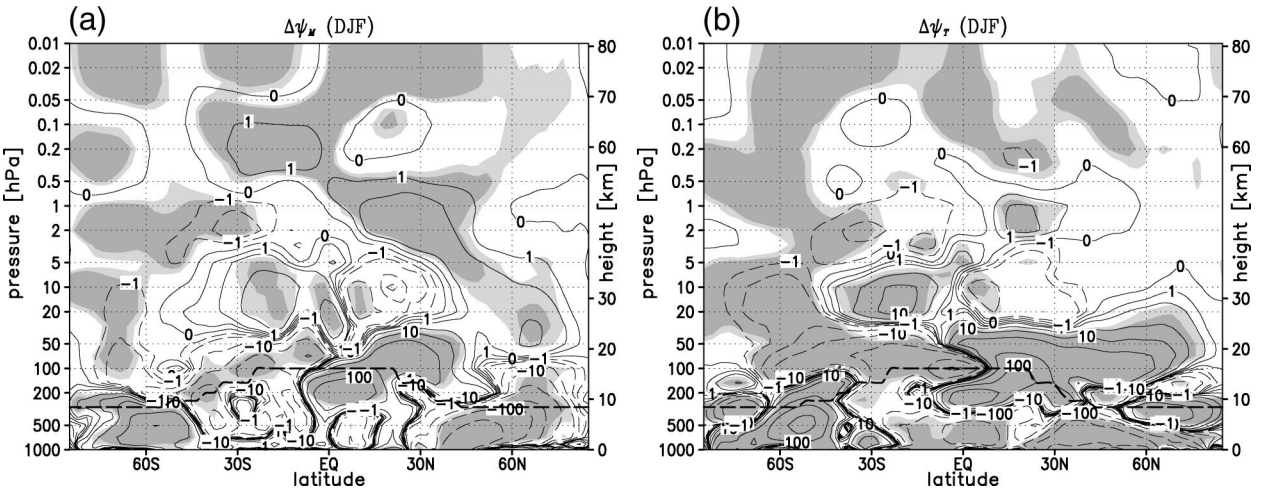

FIG. 7. As in Figs. 5a,b except for the residual streamfunction. Contour lines are at 0, ±1, ±2, ±5, ±10, ±20, ±50 kg m^{-1} s^{-1}, etc. Light (dark) shading denotes significance at 95% (99%) level of the changes.

proximately two-thirds of the increases found in the A run. Associated with this increase, the downward motions near the North Pole increase too, leading to adiabatic heating and causing the temperature increase shown in Fig. 5b. Similarly, the upward motions in the tropical lower stratosphere increase, causing adiabatic cooling and a temperature decrease in the tropical lower stratosphere. Also similar to what was found in the A run, the increased extratropical stratospheric residual circulation is driven by the increased wave driving by both resolved (planetary) waves and unresolved (gravity) waves. The effect of the resolved waves on the zonal-mean flow is quantified by div$\mathbf{F}_T/\rho_0$. The causes of Δdiv$\mathbf{F}_T/\rho_0$ (Fig. 8b) are similar to the causes of Δdiv$\mathbf{F}_A/\rho_0$ described in section 3b: the negative values of Δdiv$\mathbf{F}_T/\rho_0$ in the NH midlatitude lower stratosphere are again mainly caused by dissipation of increased upward propagating wave activity in the lower stratosphere, and the pattern of Δdiv$\mathbf{F}_T/\rho_0$ in the NH subtropical lower stratosphere and in the NH upper stratosphere is again mainly determined by changes in the meridional refraction of the planetary waves (not shown). To summarize, the patterns and causes of the middle-atmospheric changes in the T run are similar to those in the A run, with the exception that in the T run the middle-atmosphere does not cool due to the radiative effects of CO_2 doubling. The residual circulation increase in the T run is about two-thirds of the increase in the A run.

Figure 5a shows that the middle-atmosphere cools in response to middle-atmospheric CO_2 doubling, which can be explained by radiative arguments. Since the temperature responses in the Arctic lower stratosphere are additive (Fig. 5c), it is tempting to conclude that the positive ΔT_A in the Arctic stratosphere (Fig. 2a) is a small residual of a negative ΔT_M due to radiative cooling

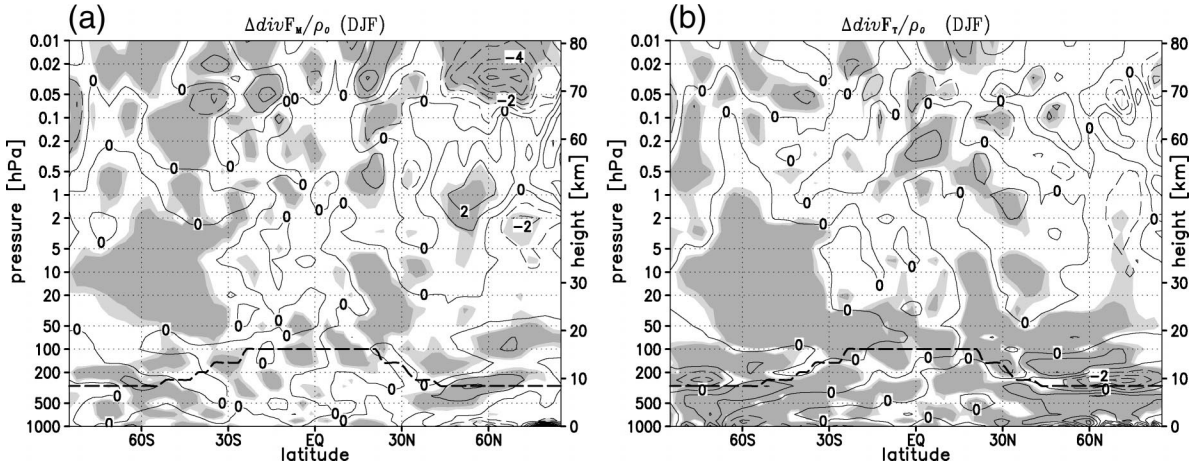

FIG. 8. As in Figs. 5a,b except for div$\mathbf{F}/\rho_0$. The contour interval is 1 m s^{-1} day^{-1}. Light (dark) shading denotes significance at 95% (99%) level of the changes.

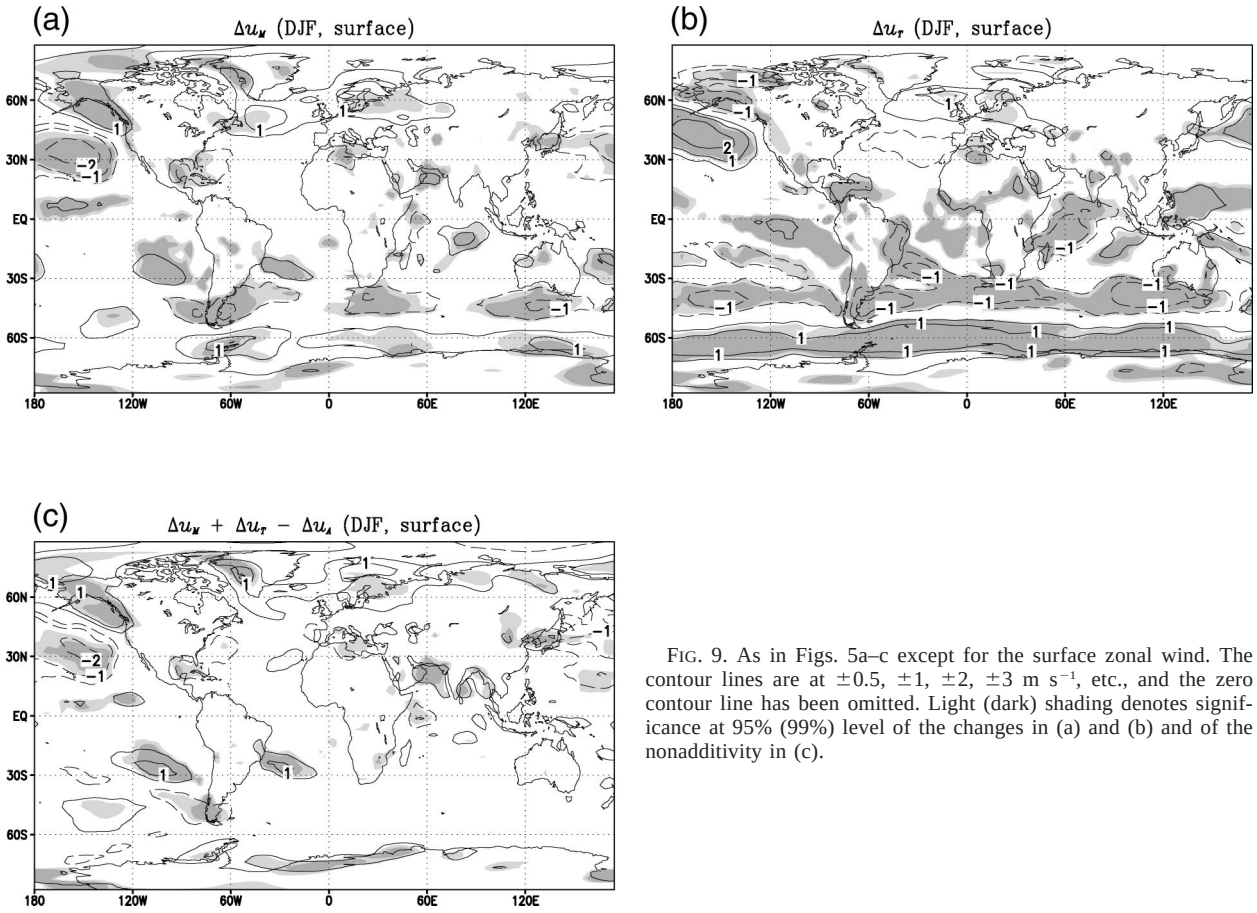

FIG. 9. As in Figs. 5a–c except for the surface zonal wind. The contour lines are at ± 0.5, ± 1, ± 2, ± 3 m s^{-1}, etc., and the zero contour line has been omitted. Light (dark) shading denotes significance at 95% (99%) level of the changes in (a) and (b) and of the nonadditivity in (c).

and a somewhat larger positive ΔT_T due to dynamical heating. However, a more detailed investigation of the responses in the M run reveals that ΔT_M itself is a result of both radiative cooling and dynamical heating. Figure 7a shows that, similar to what was found in the A run, the stratospheric residual circulation in the M run generally increases, with the exception of the tropical middle stratosphere. The amplitude of this increase is approximately one-third of that in the A run; the maximum of the residual streamfunction in the M run increases 7% at 50 hPa and 13% at 100 hPa. Similar to what was found in the A and the T runs, this increase is associated with stronger downward motions in and a warming of the Arctic lower stratosphere. Since ΔT_M is negative in this region, it can be concluded that in the M run the radiative cooling is larger than the dynamical heating. The patterns of $\Delta \text{div}\mathbf{F}_M/\rho_0$ (Fig. 8a), $\Delta \text{div}\mathbf{F}^y_M/\rho_0$ and $\Delta \text{div}\mathbf{F}^z_M/\rho_0$ (not shown) are similar to those in the T and A runs, but the amplitudes are smaller.

In summary, the simulated Arctic lower stratospheric warming in the uniformly doubled CO_2 climate is a small residual of radiative cooling and dynamical heating. The dynamical heating is caused by increased downward motions associated with the increase of the stratospheric residual circulation, which is caused by the increase of both the resolved and unresolved wave driving. The stratospheric residual circulation increase can be attributed for about two-thirds to the (remote) tropospheric CO_2 doubling and for about one-third to the (in situ) middle-atmospheric CO_2 doubling.

b. The tropospheric and surface-level response

Figure 5c shows that the tropospheric temperature changes satisfy additiveness in most regions, except in the tropical upper troposphere and the polar troposphere. Figure 6c shows that the tropospheric zonal wind changes satisfy additiveness in most regions, including the NH midlatitudes. Figure 9 shows the zonal wind responses at the surface. Figure 9c shows that the surface zonal wind responses are additive above the entire northern Atlantic. In this region, both Δu_M (Fig. 9a) and Δu_T (Fig. 9b) are positive. The zonal wind responses are not additive in large parts of the northern Pacific. In this region, the pattern of Δu_T is similar to that of Δu_A, whereas the pattern of Δu_M is completely different. In the midlatitudes of the Southern Hemisphere the zonal wind responses are additive, and the patterns of both Δu_M and Δu_T are similar to that of Δu_A.

Figure 5a shows that in the largest part of the tro-

posphere the temperature response to middle-atmospheric CO_2 doubling (ΔT_M) is small. This is not surprising since in the M run the CO_2 is not doubled in the troposphere, so direct radiative effects are absent. The tropospheric ΔT_M is characterized by a ''tongue'' of increased positive ΔT_M in both the NH and SH midlatitudes. In the NH midlatitudes Δu_M (Fig. 6a) is similar to Δu_A. The tropospheric u_M increases in the region north of 45°N. This increase is largest around 55°N and is generally statistically significant between 45° and 70°N. The amplitude of Δu_M is here comparable to that of Δu_A, implying that this tropospheric zonal wind response to middle-atmospheric CO_2 doubling is substantial. Since the zonal wind responses are nonadditive in the regions around 35° and 70°N, the negative Δu_M near 35°N and the positive Δu_M north of 65°N will not be further discussed. The poleward shift of the SH westerlies in the A run also occurs in the M run. In this region, Δu_M is about one-third of Δu_A. Figure 9a shows the surface zonal wind response to middle-atmospheric CO_2 doubling. The positive Δu_M in the western part of the northern Atlantic is statistically significant, and only slightly smaller than Δu_A (Fig. 2d). Since the surface zonal wind responses were shown to be nonadditive above the northern Pacific (Fig. 9c), the pattern of Δu_M in this region will not be discussed. The surface air temperature change in the M run (not shown) is generally smaller than 1 K. No high-latitude warming amplification is found because the sea ice distribution of the control run has been used.

Figure 5b shows that the troposphere warms in response to tropospheric CO_2 doubling, which is due to the radiative effects of the increased CO_2 concentration. In the troposphere, ΔT_T is about 80% of ΔT_A. Since the imposed SST increases in the T run are 84% of those in the A run (see section 2), this result suggests that the strength of the tropospheric warming is also influenced by the imposed SSTs. The structure of ΔT_T is similar to that of ΔT_A: the largest values (more than 5 K) occur in the tropical upper troposphere. In the NH midlatitude troposphere Δu_T (Fig. 6b) is very small and not statistically significant, in contrast to Δu_M (Fig. 6a). Since the zonal wind responses are additive in this region, this result indicates that not the tropospheric CO_2 doubling, but the remote middle-atmospheric CO_2 doubling is the main cause of the increased tropospheric NH midlatitude westerlies in the uniformly doubled CO_2 climate. It indicates that the downward influence of the middle-atmospheric CO_2 increase on the tropospheric climate is quite pronounced, at least in the NH midlatitudes. Figure 6b shows that the poleward shift of the SH westerlies also occurs in the T run. In this region, the amplitude of Δu_T is about two-thirds of that of Δu_A. As the zonal wind responses are additive in this region, this suggests that the poleward shift of the SH westerlies in the uniformly doubled CO_2 climate is mainly due to tropospheric CO_2 doubling. In contrast to the tropospheric zonal mean Δu_T, the surface Δu_T (Fig. 9b) is statistically significant in some parts of the NH midlatitudes. The surface zonal wind above the northern Atlantic increases in response to tropospheric CO_2 doubling, but this increase is only significant in a small region in the east part of the northern Atlantic. The pattern of the surface air temperature change in the T run (not shown) is very similar to that in the A run (Fig. 2e). The high-latitude warming amplification is also found in the T run because the sea ice distribution of the A run has been used.

To summarize, the middle-atmospheric CO_2 doubling causes significant increases in the tropospheric NH midlatitude westerlies, in contrast to the tropospheric CO_2 doubling. Since the zonal wind responses are additive in this region, it can be concluded that the middle-atmospheric CO_2 doubling is the main cause of the increased tropospheric NH midlatitude westerlies in the uniformly doubled CO_2 climate.

5. Additional experiments on the response of the troposphere to middle-atmospheric CO_2 doubling

In section 4b it has been shown with the M run that the middle-atmospheric CO_2 doubling causes significant increases in the tropospheric NH midlatitude westerlies during DJF. To account for the effect of the radiative forcing of middle-atmospheric CO_2 doubling on the SSTs, the imposed SST increase in the M run is 16% of that in the A run (see section 2b).

Two questions arise that will be addressed in this section:

1) Which part of the tropospheric response in the M-run is caused by the imposed SST changes, and which part is caused by the middle-atmospheric CO_2 doubling?
2) How well should the middle-atmosphere be represented in GCMs to capture the middle-atmospheric influence on the troposphere?

The first question will be addressed in section 5a, where results will be presented from an experiment (denoted as the MC run) with the same configurations as the M run, except that the control SSTs are prescribed. The second question will be addressed in section 5b, where results will be presented from an experiment in which the CO_2 is doubled only above 10 hPa. The responses found in this experiment will give an indication of how much of the middle-atmospheric CO_2 doubling influence on the troposphere is not captured in GCMs with an upper boundary around 10 hPa.

a. The tropospheric response to middle-atmospheric CO_2 doubling without change of SSTs

Figure 10a shows that the tropospheric pattern of the temperature response in the MC run (denoted as ΔT_{MC}) is similar to that in the M run (Fig. 5a) in the Northern

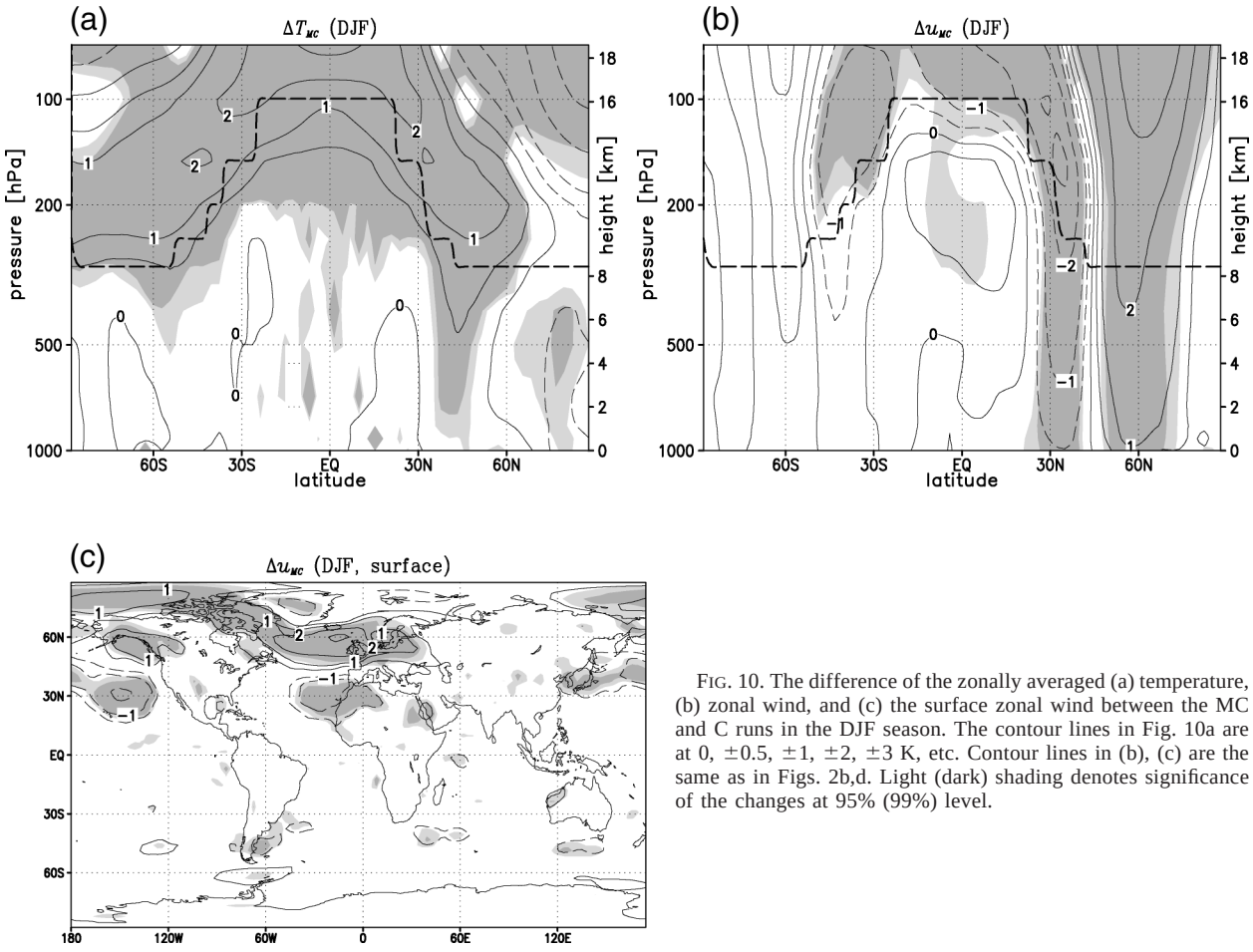

FIG. 10. The difference of the zonally averaged (a) temperature, (b) zonal wind, and (c) the surface zonal wind between the MC and C runs in the DJF season. The contour lines in Fig. 10a are at 0, ±0.5, ±1, ±2, ±3 K, etc. Contour lines in (b), (c) are the same as in Figs. 2b,d. Light (dark) shading denotes significance of the changes at 95% (99%) level.

Hemisphere, but different from that in the M run in the Southern Hemisphere: in the MC run the tongue of increased temperatures is only found in the Northern Hemisphere. The ΔT_{MC} is 0.3–1 K smaller than ΔT_M. These results show that the imposed SST changes in the M run cause a rather uniform tropospheric warming and a tongue of additional warming in the SH midlatitudes. Similar conclusions can be drawn for the tropospheric zonal wind (Fig. 10b): the significant midlatitude zonal wind increases in the M run only occur in the MC run in the midlatitudes of the Northern Hemisphere. The tropospheric Δu_{MC} is even larger than the Δu_M, suggesting that in the M run the imposed SSTs weaken the tropospheric zonal wind response to middle-atmospheric CO_2 doubling. Similar results are found for the surface zonal wind: above the northern Atlantic the surface Δu_{MC} (Fig. 10c) is about twice larger than the surface Δu_M. It can thus be concluded that, in the M run, the increased NH westerlies are not caused by the imposed SSTs, but by the middle-atmospheric CO_2 doubling. From this result and the results presented in section 4b, it can be concluded that the middle-atmospheric CO_2 doubling and not the imposed SSTs or tropospheric CO_2 doubling is the main cause of the increased NH westerlies in the uniformly doubled CO_2 climate. On the other hand, the poleward shift of the SH westerlies in the M run is not found in the MC run, suggesting that the SH response in the M run is caused by the imposed SST changes. It is concluded that not the middle-atmospheric CO_2 doubling, but the tropospheric CO_2 doubling and the imposed SSTs cause the poleward shift of the SH midlatitude westerlies in the uniformly doubled CO_2 climate.

b. The tropospheric response to CO_2 doubling above 10 hPa

Now that it has been demonstrated that the middle-atmospheric CO_2 doubling is important for the tropospheric and surface climate response in the uniformly doubled CO_2 climate, one may wonder how well the middle-atmosphere has to be represented in GCMs to capture this downward influence. As described in section 1, several authors have addressed the issue of how high the model top should be to produce realistic climate simulations. Gillett et al. (2002) and Shindell et al. (1999) compared the AO responses to increasing greenhouse gases in a high (upper boundary around 0.01 hPa)

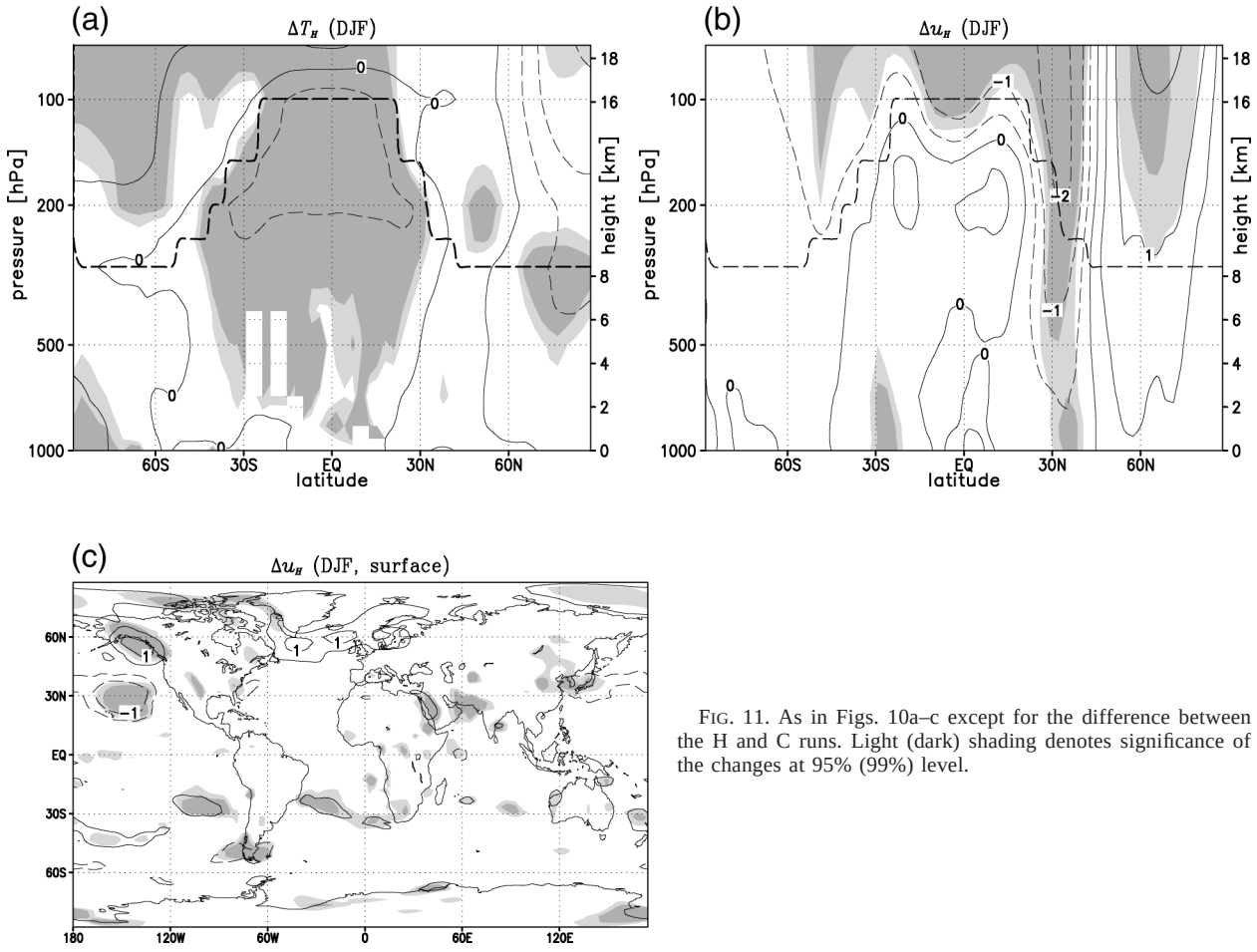

FIG. 11. As in Figs. 10a–c except for the difference between the H and C runs. Light (dark) shading denotes significance of the changes at 95% (99%) level.

and a low (upper boundary around 10 hPa) version of their models, and found contrasting results. Rind et al. (1998) also addressed the model top question and found that the stratospheric responses to doubled CO_2 in models with model tops at 0.01 and 1 hPa are similar. Instead of investigating the required minimum model top height for producing reliable climate predictions, here we address a slightly different issue. An additional run has been performed in which the CO_2 is doubled between 10 and 0.01 hPa to investigate directly the influence of CO_2 changes above 10 hPa on the surface climate. SSTs from the control run are imposed in this run, which will be referred to as the H run.

Figure 11a shows that the tropospheric temperature response to CO_2 doubling above 10 hPa (ΔT_H) is generally small. The tropospheric zonal wind response in the NH midlatitudes (Δu_H, Fig. 11b) is surprisingly large: Δu_H is not much smaller than Δu_M (Fig. 6a) and about 50% of Δu_{MC} (Fig. 10b). As in the M and MC runs, the zonal wind decreases significantly around 35°N. The zonal wind in the SH troposphere does not change significantly in the H run. The structure of the surface Δu_H is again similar to that of Δu_{MC} (Fig. 10c) and Δu_M (Fig. 9a), whereas the amplitude is slightly smaller than the amplitude of Δu_M and about 50% of the amplitude of Δu_{MC}. These results suggest that CO_2 doubling above 10 hPa significantly contributes to the strengthening of the tropospheric NH midlatitude westerlies in the uniformly doubled CO_2 climate.

6. Discussion and conclusions

In this paper, the separate climate effects during NH winter of tropospheric and middle-atmospheric CO_2 doubling have been studied with the middle-atmosphere version of the ECHAM global climate model. It has been investigated to what extent the changes in the uniformly doubled CO_2 climate can be considered as the sum of the separate tropospheric and middle-atmospheric CO_2 doubling responses. Thereafter, changes in the uniformly doubled CO_2 climate have been attributed to either tropospheric or middle-atmospheric CO_2 doubling. In addition, the question of how well the middle-atmosphere has to be represented in GCMs to acquire reliable tropospheric climate predictions has been addressed.

Since planetary waves originating from the troposphere are dissipated in the stratosphere and drive a

meridional circulation and the stratosphere is thought to exert a significant downward influence on the troposphere, the coupling between the middle-atmosphere and the troposphere is anticipated to be important for understanding the changes in the doubled CO_2 climate (section 1). In the doubled CO_2 climate the Arctic lower stratosphere slightly warms, causing a decrease of the meridional temperature gradient and, consequently, a weakening of the Arctic middle-atmospheric zonal wind (section 3). The small warming is thought to be caused by increased downward motions associated with an increased residual circulation. In the Arctic lower stratosphere the temperature response in the uniformly doubled CO_2 climate can be regarded as the sum of the responses to CO_2 doubling in the middle-atmosphere and in the troposphere. The increased residual circulation contributing to the small Arctic lower stratospheric warming in the uniformly doubled CO_2 climate can be attributed for about two-thirds to the tropospheric CO_2 doubling and about one-third to the middle-atmospheric CO_2 doubling (section 4a). These results are consistent with those presented by Rind et al. (1990), who with much shorter experiments found that both middle-atmospheric and tropospheric CO_2 doubling contribute to the increase of the residual circulation. However, the increase of the stratospheric residual circulation and the resulting dynamical heating due to ''in situ'' middle-atmospheric CO_2 doubling is probably larger in their study. In their STRAT run, which can be compared to our M run, the dynamical heating due to the stratospheric residual circulation increase exceeds the radiative cooling, resulting in an upper-stratospheric warming (their Fig. 4). In our M run the dynamical heating is smaller than the radiative cooling, resulting in a cooling in the entire middle-atmosphere (Fig. 5a). However, the STRAT run was integrated for one winter, whereas our M run was integrated for 30 years. Therefore, the different results may be due to model differences, but also due to differences in the length of the integration.

In the uniformly doubled CO_2 climate the tropospheric NH midlatitude westerlies increase and the SH westerlies shift poleward (section 3). The zonal wind responses were shown to be additive in these regions. The increased tropospheric NH midlatitudes westerlies are mainly caused by the (remote) middle-atmospheric CO_2 doubling and not by the tropospheric CO_2 doubling (section 4b). The middle-atmosphere contains only $\sim$15% of the total atmospheric mass. If we consider the zonal wind response in terms of response per kg CO_2 increase, the zonal wind response to middle-atmospheric CO_2 doubling is even more dominant over that due to tropospheric CO_2 doubling. In contrast, the poleward shift of the SH tropospheric westerlies has been attributed to the tropospheric CO_2 doubling.

It has been concluded that in NH winter the middle-atmospheric CO_2 doubling has an important effect on the NH tropospheric climate change. The question of how well the middle-atmosphere has to be represented in GCMs to capture this downward influence has been addressed in section 5b. It has been shown that CO_2 doubling above 10 hPa already causes significant increases of the tropospheric NH midlatitude westerlies.

The question of which mechanisms are responsible for the downward influence of the middle-atmosphere in the doubled CO_2 climate is still under debate. Shindell et al. (1999) argue that the change in the meridional temperature gradient in the midlatitude tropopause region in response to increasing greenhouse gases causes changes in the stratospheric circulation that could influence the tropospheric circulation through wave–mean flow interactions. The attribution of the tropospheric NH midlatitude zonal wind increase to middle-atmospheric CO_2 doubling, and the attribution of the poleward shift of the tropospheric SH summer westerlies to tropospheric CO_2 doubling are consistent with this hypothesis. The middle-atmospheric zonal wind in NH winter is easterly in the SH, constituting a barrier for the transport of tropospheric wave activity into the middle-atmosphere (Charney and Drazin 1961). Because of the lack of wave activity in the middle-atmosphere, the middle-atmosphere cannot influence the tropospheric climate through wave–mean flow interactions. Therefore, the changes in the SH summer troposphere in the doubled CO_2 climate are expected to be the result of changes in the troposphere itself, and not from the coupling with the middle-atmosphere. In the Northern Hemisphere winter, the NH middle-atmospheric zonal wind is westerly, allowing tropospheric wave activity to propagate into the stratosphere, which, through wave–mean flow interactions can influence the troposphere. Shindell et al. (1999) found a strengthening of the Arctic vortex in response to increasing greenhouse gases and argued that it induces a strengthening of the (lower) tropospheric westerlies through wave–mean flow interactions. Our results do not support this argument since we also find a strengthening of the tropospheric NH midlatitude westerlies, but a weakening of the stratospheric Arctic zonal winds [both results are also found in other models, see Gillett et al. (2003)]. This does not contradict the hypothesis that the tropospheric NH midlatitude zonal wind changes are induced by stratospheric zonal wind changes through wave–mean flow interactions, but the exact mechanism remains unclear.

In summary, in this paper the importance of the tropospheric climate change for the increase of the stratospheric residual circulation and associated middle-atmospheric responses (small Arctic lower stratospheric warming and weakening of zonal wind in the Arctic middle-atmosphere) in the uniformly doubled CO_2 climate has been shown. In addition, the results indicate the crucial role of the middle-atmospheric climate change in the increase of the tropospheric NH midlatitude westerlies in the uniformly doubled CO_2 climate. Finally, the need to include the region above 10 hPa in GCMs to acquire realistic climate predictions has been advocated.

Acknowledgments. The authors would like to thank Hans Cuijpers (KNMI) for extensive model support, Peter van Velthoven and Rob van Dorland (both KNMI), Frans Sluijter (Eindhoven University of Technology), and Neal Butchart and Adam Scaife (both U.K. Meteorological Office) for helpful comments and suggestions, Kleareti Tourpali (University of Thessaloniki) for providing the tropopause climatology, and Erich Roeckner (Max-Planck-Institut für Meteorologie) for providing the SST climatologies for the C and A run. Comments of two anonymous reviewers helped improve the manuscript, and are greatly appreciated.

REFERENCES

Andrews, D. G., J. R. Holton, and C. B. Leovy, 1987: *Middle Atmosphere Dynamics.* Academic Press, 490 pp.

Baldwin, M. P., and T. J. Dunkerton, 1999: Propagation of the Arctic Oscillation from the stratosphere to the troposphere. *J. Geophys. Res.,* **104,** 30 937–30 946.

Boville, B. A., 1984: The influence of the polar night jet on the tropospheric circulation in a GCM. *J. Atmos. Sci.,* **41,** 1132–1142.

Brühl, C., 1993: Atmospheric effects of stratospheric aircraft. Report of the 1992 Models and Measurements Workshop, NASA Ref. Publ. 1292 II, VII, 240 pp.

Butchart, N., and A. A. Scaife, 2001: Removal of chlorofluorocarbons by increased mass exchange between the stratosphere and troposphere in a changing climate. *Nature,* **410,** 799–802.

Charney, J. G., and P. G. Drazin, 1961: Propagation of planetary-scale disturbances from the lower into the upper atmosphere. *J. Geophys. Res.,* **66,** 83–109.

Fels, S. B., J. D. Mahlman, M. D. Schwarzkopf, and R. W. Sinclair, 1980: Stratospheric sensitivity to perturbations in ozone and carbon dioxide: Radiative and dynamical response. *J. Atmos. Sci.,* **37,** 2265–2297.

Fyfe, J. C., G. J. Boer, and G. M. Flato, 1999: The Arctic and Antarctic Oscillations and their projected changes under global warming. *Geophys. Res. Lett.,* **26,** 1601–1604.

Gillett, N. P., M. R. Allen, and K. D. Williams, 2002: The role of stratospheric resolution in simulating the Arctic Oscillation response to greenhouse gases. *Geophys. Res. Lett.,* **29,** 1500–1503.

——, ——, and ——, 2003: Modelling the atmospheric response to doubled CO_2 and depleted stratospheric ozone using a stratosphere-resolving coupled GCM. *Quart. J. Roy. Meteor. Soc.,* **129,** 947–966.

Hartley, D. E., J. Villarin, R. X. Black, and C. A. Davis, 1998: A new perspective on the dynamical link between the stratosphere and troposphere. *Nature,* **391,** 471–474.

Haynes, P. H., C. J. Marks, M. E. McIntyre, T. G. Shepherd, and K. P. Shine, 1991: On the ''downward control'' of extratropical diabatic circulation by eddy-induced mean zonal forces. *J. Atmos. Sci.,* **48,** 651–678.

Hines, C. O., 1997a: Doppler spread parameterization of gravity wave momentum deposition in the middle-atmosphere. Part 1: Basic formulation. *J. Atmos. Sol. Terr. Phys.,* **59,** 371–386.

——, 1997b: Doppler spread parameterization of gravity wave momentum deposition in the middle-atmosphere. Part 2: Broad and quasi-monochromatic spectra and implementation. *J. Atmos. Sol. Terr. Phys.,* **59,** 387–400.

Holton, J. R., P. H. Haynes, M. E. McIntyre, A. R. Douglass, R. B. Rood, and L. Pfister, 1995: Stratosphere–troposphere exchange. *Rev. Geophys.,* **33,** 403–439.

Houghton, J. T., Y. Ding, D. J. Griggs, M. Noguer, P. J. van der Linden, and D. Xiaosu, 2001: *Climate Change 2001: The Scientific Basis.* Cambridge University Press, 944 pp.

Kodera, K., K. Yamazaki, M. Chiba, and K. Shibata, 1990: Downward propagation of upper stratospheric mean zonal wind perturbation to the troposphere. *Geophys. Res. Lett.,* **17,** 1264–1266.

Mahfouf, J. F., D. Cariolle, J. F. Royer, J. F. Geleyn, and B. Timbal, 1994: Response of the Meteo-France climate model to changes in CO_2 and sea surface temperature. *Climate Dyn.,* **9,** 345–362.

Manzini, E., and N. A. McFarlane, 1998: The effect of varying the source spectrum of a gravity wave parameterization in a middle-atmosphere general circulation model. *J. Geophys. Res.,* **103,** 31 523–31 539.

——, ——, and C. McLandress, 1997: Impact of the Doppler spread parameterization on the simulation of the middle-atmosphere circulation using the MAECHAM4 general circulation model. *J. Geophys. Res.,* **102,** 25 751–25 762.

McFarlane, N. A., 1987: The effect of orographically exited gravity wave drag on the general circulation of the lower stratosphere and troposphere. *J. Atmos. Sci.,* **44,** 1775–1800.

Paeth, H., A. Hense, R. Glowienka-Hense, S. Voss, and U. Cubasch, 1999: The North Atlantic Oscillation as an indicator for greenhouse-gas induced regional climate change. *Climate Dyn.,* **15,** 953–960.

Rind, D., R. Suozzo, N. K. Balachandran, and M. J. Prather, 1990: Climate change and the middle-atmosphere. Part I: The doubled CO_2 climate. *J. Atmos. Sci.,* **47,** 475–494.

——, D. Shindell, P. Lonergan, and N. K. Balachandran, 1998: Climate change and the middle-atmosphere. Part III: The doubled CO_2 climate revisited. *J. Climate,* **11,** 876–894.

——, P. Lonergan, N. K. Balachandran, and D. Shindell, 2002: $2 \times CO_2$ and solar variability influences on the troposphere through wave–mean flow interactions. *J. Meteor. Soc. Japan,* **80,** 811–830.

Roeckner, E., and Coauthors, 1996: The atmospheric general circulation model ECHAM4: Model description and simulation of present day climate. Max-Planck Institute for Meteorology Rep. 218, Hamburg, Germany, 90 pp.

Rosenlof, K. H., and J. R. Holton, 1993: Estimates of the stratospheric residual circulation using the downward control principle. *J. Geophys. Res.,* **98,** 10 465–10 479.

Shindell, D. T., D. Rind, and P. Lonergan, 1998: Increased polar stratospheric ozone losses and delayed eventual recovery owing to increasing greenhouse-gas concentrations. *Nature,* **392,** 589–592.

——, R. L. Miller, G. Schmidt, and L. Pandolfo, 1999: Simulation of recent northern winter climate trends by greenhouse-gas forcing. *Nature,* **399,** 452–455.

——, G. A. Schmidt, R. L. Miller, and D. Rind, 2001: Northern Hemisphere winter climate response to greenhouse gas, ozone, solar, and volcanic forcing. *J. Geophys. Res.,* **106,** 7193–7210.

Sigmond, M., P. C. Siegmund, and H. Kelder, 2003: Analysis of the coupling between the stratospheric meridional wind and the surface level zonal wind during 1979–93 Northern Hemisphere extratropical winters. *Climate Dyn.,* **21,** 211–219.

Thompson, D. W. J., and J. M. Wallace, 1998: The Arctic Oscillation signature in the wintertime geopotential height and temperature fields. *Geophys. Res. Lett.,* **25,** 1297–1300.

——, ——, and G. C. Hegerl, 2000: Annular modes in the extratropical circulation. Part II: Trends. *J. Climate,* **13,** 1018–1036.